JOURNAL OF AIRCRAFT
Vol. 35, No. 5, September–October 1998

Modal Technique for Active Control of Tones Radiated from a Ducted Fan

Tatsuya Ishii,* Hiroshi Kobayashi,† and Hideshi Oinuma‡
National Aerospace Laboratory, Tokyo 182-8522, Japan

This paper describes research in the development of a modal technique considered appropriate for the active noise control (ANC) of fan tones. Two essential issues were addressed to establish this technique. The first was to develop a waveform generation system, which can produce the arbitrary spinning modes necessary for tone cancellation. The second was to develop a modal detection system for the spinning modes. An examination of two systems showed that the desired spinning modes in the circumferential direction of a duct could be produced, and that the contents of the acoustic spinning modes in the duct could be determined with a high accuracy. A technological assessment of the modal technique composed of the two systems was challenged using a ducted fan. At a fan speed of 4125 rpm, the noise reduction in the blade-passage frequency could be achieved ranging from 2 to 10 dB without spillover caused by a secondary sound source. Although these experimental results are limited, they suggest that the modal technique for ANC of acoustic spinning modes in fan tones may be feasible. Additional technical issues such as the simultaneous noise reduction of higher harmonics and the sound power needed for the secondary sound sources should be resolved for further noise reduction.

I. Introduction

THE noise caused by an engine fan or compressor on take-off and approach has become a major component of the noise of higher bypass ratio turbofan engines. Reducing the fan or compressor noise radiating from aeroengines, gas turbines, and air blowers will contribute to providing a better living and work environment. In an inlet fan duct, rotor alone and rotor/stator interactions generate a pressure field in the form of acoustic spinning modes.[1,2] Attenuating these spinning modes is one of the effective ways to weaken the noise radiated from a fan or a compressor. This is because the acoustic power of spinning mode is high enough and can never be ignored compared with other noise components, such as broadband noise.

The spinning modes in the duct can be detected experimentally[3–7] and this information can be used to design an optimum acoustic lining. However, in the case of high bypass ratio or ultrahigh bypass ratio turbofan engines, there are two difficulties that arise in traditional acoustic treatments for reducing fan tones. The first is that a larger fan generates lower-frequency tones. For attenuating lower-frequency tones, the acoustic lining requires a larger volume. This requirement leads to an increase in engine weight and the deterioration of engine nacelle performance. Another difficulty is that the nacelle area available for acoustic lining is decreasing to minimize the weight. Because of these difficulties, a new approach is required for engine noise reduction that has less weight, a low power requirement, a sufficient noise reduction, and a quick response to changes in engine operating conditions.

Active noise control (ANC) includes developing technologies that satisfy the preceding demands. To achieve ANC for fan noise, several methods have been proposed and examined experimentally and theoretically in recent years.[8–11] The results of these studies have shown some noise reduction of fan tones. Actuators and sensors have also been designed and tested.[12] The ANC test of Ref.13 has demonstrated that for a ducted fan, controlling the spinning mode results in fan noise reduction.[13] Technological difficulties remain, however, which must be overcome to ensure further progress.

One of the difficulties is spillover because of the distributed secondary sound sources. Secondary sound adds to noise instead of reducing it, if the secondary sound is not in opposite phase to noise. The ANC of spinning modes requires not only adjusting the phase of the secondary sound to that of noise, but also fitting modes of the secondary sound to those of noise. Another difficulty is the acoustic power required for the secondary sound source to cancel the noise. In former studies,[9,10] the fan speed was restricted low enough because of the lack in acoustic power of loud speakers. The smaller and more efficient sound source is desired.

As for the control principle, we adopted a waveform synthesis to avoid the spillover and to respond to arbitrary spinning modes because it is capable of generating arbitrary antiphased spinning modes in the duct.[14,15] Because of assuming consistent modal structure, the waveform synthesis is expected to demonstrate stable ANC performance against small disturbances, whereas the time-dependent ANC method sometimes suffers from disturbances caused by fluctuating fan speed or inflow noise. The technique necessary for the waveform synthesis is divided into two parts. The first is a technique to detect the acoustic modal structures caused by a fan assembly. The modal structure is determined by use of acoustic measurement in the duct. For the measurement, we prepared a flush-mounted microphone array on the duct surface and a probe microphone movable anywhere across the duct cross section. The second part is a technique to compose spinning modes the same as those obtained by the modal detection and to release the composed spinning modes with an antiphase relative to noise.

II. Test Facility

A schematic view of the test facility is shown in Fig. 1. The facility is composed of a waveform generation system, a modal detection system, a ducted fan, and an anechoic room.[16] Figure 2 shows photographs of the test facility viewed from inside and outside the anechoic room.

Received Sept. 8, 1997; revision received May 25, 1998; accepted for publication May 29, 1998.

*Researcher, Advanced Noise Control Research Group. Member AIAA.
†Leader, Advanced Noise Control Research Group. Member AIAA.
‡Researcher, Advanced Noise Control Research Group.

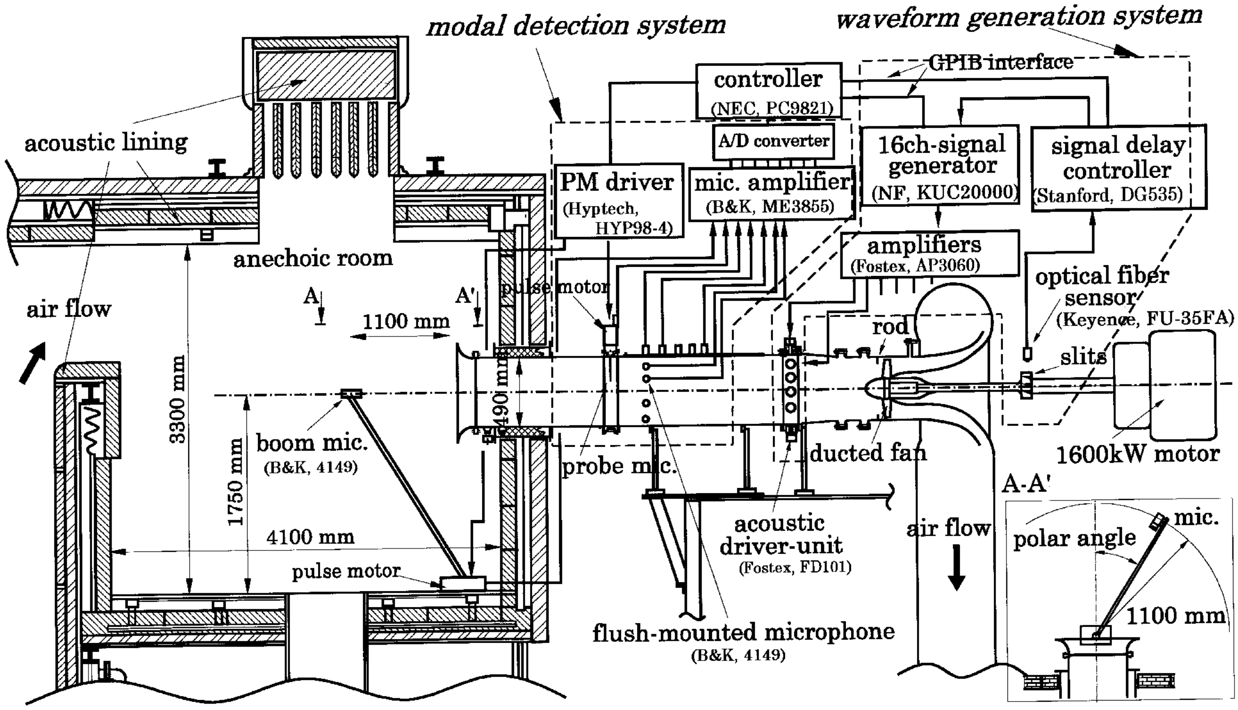

Fig. 1 Schematic view of ANC test facility.

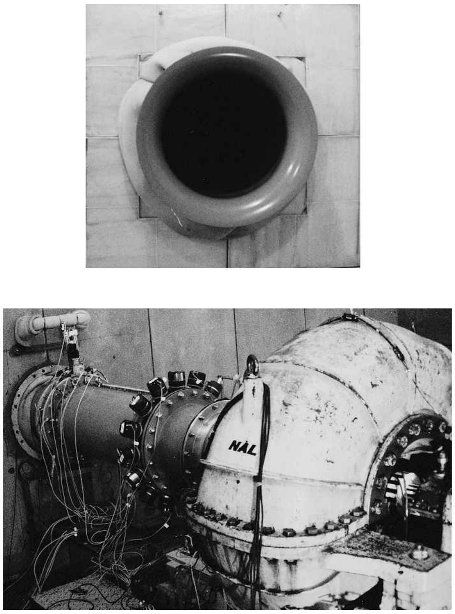

a)

b)

Fig. 2 Photos viewed from a) inside and b) outside the anechoic room.

A. Waveform Generation System

The waveform generation system is designed to generate spinning modes in an antiphase to spinning modes caused by the noise source. The system is divided into two parts and applied to a duct with a diameter of 490 mm and a length of 2700 mm, as illustrated in Fig. 1.

The one part consists of a 16-channel signal generator, a 16-channel amplifier, and 16 acoustic driver units. The 16-channel signal generator is capable of repeatedly transmitting an arbitrary signal to each channel and adjusting the amplitude, the phase relative to an external input, and the modes of each output signal. By inputting external signal, one can synchronize all output signals of the signal generator in response to the external trigger signal. Each output signal is amplified and inputted to the corresponding acoustic driver unit. Each acoustic driver unit is installed at an equal interval in the circumferential direction of the duct.

The other part of the system has an optical fiber sensor and a signal-delay controller. The fiber sensor counts the passage of slits painted on the fan shaft. The signal triggered by the slit passage is inputted to the signal-delay controller, where the output signal can be delayed arbitrarily relative to the input signal. Because the number of slits is the same as the number of fan blades, the preceding procedures correspond to adjusting the delay relative to a blade motion. By adjusting the delay and sending the delayed signal to the external input of the signal generator, antiphased spinning modes can be generated with a desired delay to the noise source. A personal computer communicates with the signal generator and the signal-delay controller through the general-purpose interface bus (GPIB) and controls the waveform generation system.

B. Modal Detection System

A modal detection system determines the acoustic modal structures of the spinning modes in the duct through sound measurement and modal analysis. The two procedures are conducted to detect the spinning modes. At first, a microphone array acquires acoustic data at the inner surface of the duct. Microphones are flush-mounted on the duct surface axially as well as circumferentially to detect both radial modes and circumferential modes. The axial interval of the flush-mounted position is 25 mm, and the circumferential interval is 10 deg. The positions of flush-mounted microphones are selected according to the contents of spinning modes predicted by the test parameters such as fan speeds. Next, the modal analysis is conducted by solving a modal matrix. The matrix is composed of mode's complex amplitudes at each measurement position. A flush-mounted microphone position is defined by circumferential degrees on the duct surface, θ, and axial distance from the reference position on the duct, x. At the ith measurement position, (θ_i, x_i), the matrix's component of the lth spinning mode is expressed as

$$A_{i,l} = E_m(\kappa_l \cdot R) \cdot e^{j(k_x \cdot x_i + m \cdot \theta_i)} \tag{1}$$

Here, $E_m(\kappa_l \cdot R)$ is composed of m order's first and second Bessel functions at the radius of the duct, R. The index, m, means the lobe number of the lth spinning mode. In this case, $E_m(\kappa_l \cdot R)$ contains only the first Bessel function because of zero hub-tip ratios. The value, k_l, is the wave number of the lth spinning mode, which is calculated using the duct diameter. The wave number in the axial direction is denoted by k_x.[1,5] At the ith measurement position, the cross spectra relative to the reference microphone provide complex amplitude, C_i, at the concerning tone frequency. The unknown complex amplitude of the lth spinning mode, X_l, is obtained by solving the equation[5]

$$(A_{i,l}) * [X_l] = [C_i] \tag{2}$$

The waveform of the detected spinning modes is reproduced referring to the solution of modal analysis, $[X_l]$.

The performance of the modal detection system could be evaluated by comparing the waveform of detected spinning modes with that measured by the probe microphone. A combination of a circumferentially movable ring and a radial traversing probe enables the measurement position to locate anywhere in the duct cross section. We measured in advance the acoustic response of the probe itself by imposing white noise and corrected the measured spectrum. Two acoustic signals are acquired simultaneously at each measurement position. One signal is measured by the probe microphone at each measurement position. The other signal is measured by a flush-mounted microphone fixed at a certain position, namely a reference microphone. By analyzing the cross spectra obtained by the probe microphone and the reference microphone, we could obtain the amplitude and the phase of the signal at the measurement position relative to the signal at the reference microphone.

C. Ducted Fan

A ducted fan used for the noise source has 16 swept blades made from fiber-reinforced plastics and it was powered by a dc motor. The performance of the motor and the shaft danger speed restrict the maximum fan speed, 9300 rpm, which corresponded to a blade-passage frequency (BPF) of 2480 Hz. In the present tests, to obtain the spinning mode having the fewest lobes at a lower fan speed, 15 rods were placed upstream of the fan. The rods, which were 10 mm in diameter and 25% of the blade span in length, were inserted from the duct inner surface. The rods were arranged at equal intervals on the circumferential positions of the duct. Spinning modes with one lobe, two lobes, or more were expected to be strongly excited. Taking the cutoff frequency of the spinning modes and the acoustic power of the secondary sound source into consideration, the fan speed is set to 3000–5500 rpm. This corresponds to a BPF of 800–1467 Hz.

D. Anechoic Room

For measuring the sound pressure level (SPL) radiated from the duct inlet, an anechoic room with dimensions of 5700 × 4100 × 3300 mm was used. This room is anechoic above 400 Hz, and it is equipped with a boom microphone. The boom microphone traverses the 1100-mm radius polar circle centered at the duct inlet. The effect of obstacles or cavities in the radiation path limits the radius for traversing the microphone. Because the radius may not be adequate for far-field measurement, the data obtained by the boom microphone provides the radiated sound pressure levels with and without ANC to demonstrate the ANC performance.

The room contains the large cavities of an inlet silencer and a ceiling outlet silencer. It is possible that these cavities affect the flow into the fan. By traversing a hot-wire anemometer across the duct cross section, we examined the influence of inlet flow distortion and inflow turbulence. The turbulence level was measured at eight circumferential positions of the duct with the probe traversed in the radial direction at each position, and proved to be less than 3% of steady flow at all measurement positions.

III. Tests of Waveform Generation and Modal Detection

We carried out tests of waveform generation and modal detection using the systems mentioned earlier. The test is conducted through three steps. At first, a spinning mode is selected and the waveform generation system produces the spinning mode in the duct. During this test, to avoid reflection, acoustic lining at the end closed the duct end that faced the model fan. Next, the modal detection system measured sound propagating through the duct by both a flush-mounted microphone array and a probe microphone. Finally, the measured data were analyzed and the waveform of the spinning mode was determined. The determined waveform was compared with the waveform obtained by the probe microphone. The waveform by traversing the probe microphone was used as reference data in this test because the inner acoustic distribution could be measured only by the probe traversing.

A. Test Parameters

The test parameters for the generation and detection of spinning modes are shown in Table 1. The waveform generation system can produce spinning modes with 1–7 lobes using 16 acoustic driver units. The amplitude and the phase-difference imposed on each acoustic driver unit are adjusted to generate a spinning mode. The phase-difference between the adjacent driver units is given as

$$\phi_m = (360 \times m)/16 \quad (m = \pm 1, \pm 2, \pm 3, \ldots) \tag{3}$$

where m represents the number of lobes and the direction of the spin. The driving frequency of the spinning mode was selected to be from 1000 to 4500 Hz. Because higher driving frequencies might excite higher orders of radial modes, it is essential to try the modal detection at higher frequencies to ensure the system's performance to detect the spinning modes in both the circumferential and radial directions.

Table 1 Test parameters for generation and detection of spinning modes

Lobe number	Phase difference, deg	Driving frequencies, Hz
1	22.5	1000
		1500
		2000
		3000
2	45.0	1000
		2000
		2500
		3500
3	67.5	1500
		2000
		3000
		3500
4	90.0	1500
		2500
		3500
5	112.5	2500
		3500
		4000
6	135.0	2000
		2700
		3500
		4500
7	157.5	2000
		2500
		3000
		4000

B. Tests for the Generation of Spinning Modes

The SPL and the phase relative to the reference microphone were measured by the probe microphone at the duct inner surface and plotted in Fig. 3a. The driving frequency was set at 1500 Hz, and a spinning mode with four lobes was excited. The SPL is shown in top part of Fig. 3a. The lower part of Fig. 3a plots the distribution of phase delay relative to the reference microphone, which is obtained by analyzing the cross spectra between the probe microphone and the reference microphone. In Fig. 3b, the radial distribution of the sound is plotted based on data obtained when the probe is traversed radially at a chosen circumferential position. The solid line represents a Bessel function fitted to the experimental data. While the driving frequency is low enough, experimental data agree with the acoustic theory because the component concerned is limited to the (4,0) mode.

Two distinctive features to spinning modes can be observed in Fig. 3a. One is the uniform circumferential distribution of SPL. Unlike the standing wave, no nodes of SPL exist circumferentially. Another feature is seen in the phase delay distribution, which indicates a linear phase change. The linear phase change expresses the rotation of a pressure distribution in the duct. All parameters listed on Table 1 were investigated and it was confirmed that the waveform generation system is capable of generating spinning modes with mode orders and amplitudes required for ANC of the ducted fan.

In Fig. 4, instantaneous pressure distributions measured over a quarter section of the duct using a probe microphone are displayed together with a grid used for traversing. Arrows from the right to left side indicate the maximum values, and those from the left to right side indicate minimum values in each distribution. Spinning modes with four lobes can be observed

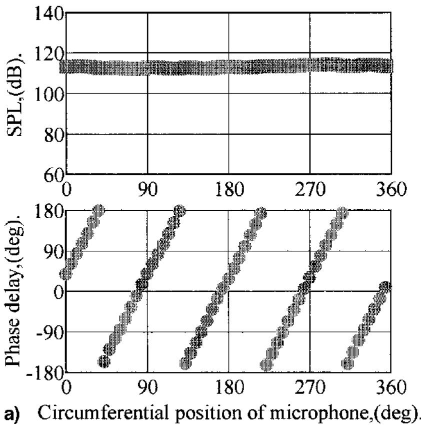

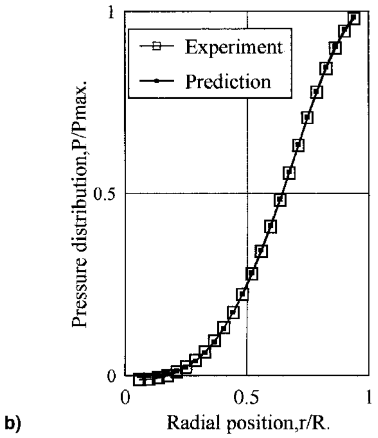

Fig. 3 a) Measured distributions of amplitude and phase in the circumferential direction at the duct inner wall. b) Measured pressure distribution in the radial direction. Driving frequency is 1500 Hz and spinning mode order is 4.

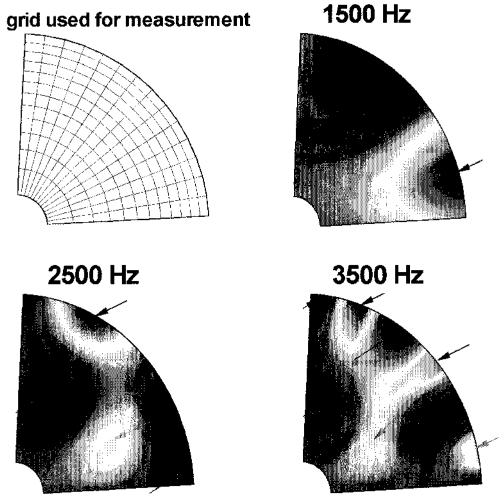

Fig. 4 Instantaneous pressure distributions of spinning modes measured by a traversing probe microphone and the grid use for measurement.

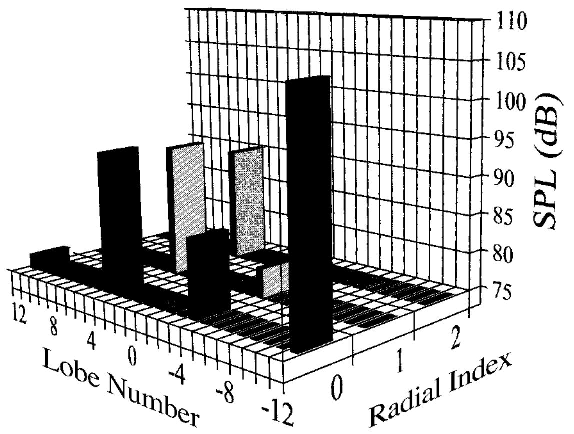

Fig. 5 Results of modal decomposition applied to the spinning modes with 3500 Hz of the driving frequency and 90 deg of the phase difference between adjacent driver units.

along the duct inner surface in the 1500 and 2500 Hz driving frequencies. As the driving frequency increases, the nodes in the radial direction become clear because the spinning modes contain higher-order radial modes. At 3500 Hz, more than four lobes seem to appear in the whole cross section. The result of the modal decomposition shown in Fig. 5 indicates the effect of the alliancing that the spinning mode with 12 lobes is excited strongly. The driving frequency of the secondary sound source must be restricted low to avoid the alliancing as well as the undesired spinning modes with higher radial modes. Considering operating conditions of the model fan, the driving frequency is limited to be less than 1500 Hz, which is assumed low enough for preventing alliancing.

C. Tests for Modal Detection by Flush-Mounted Microphones

Although flush-mounted microphones for modal detection are advantageous in that they do not affect the flowfield inside the duct, the lack of measurement in the radial direction should be compensated by the modal analysis. The modal detection test using flush-mounted microphones consists of three procedures. First, a desired spinning mode is produced by the waveform generation system according to the test parameters listed in Table 1. Next, the microphone array located at the duct inner wall measures the spinning mode that propagates through the duct. Finally, the modal structure is determined by modal analysis with measured data and the instantaneous pressure distribution across the duct is predicted based on the determined modal structure.

The predicted instantaneous pressure distribution is compared to the reference distribution obtained by the traversing probe microphone, which suggests how accurately the spinning modes were detected. An example of modal decomposition by flush-mounted microphones is displayed in Fig. 6. The parameters for the spinning mode with one lobe were set for the ANC tests. The driving frequency was set to 2000 Hz, at which the (1,0), (1,1), and (1,2) modes propagate in the duct. In Fig. 7, the instantaneous pressure distribution predicted by the modal decomposition result is shown on the right side with the reference distribution at the center of the figure. The difference between the two distributions is plotted on the left side.

On both distributions, the peaks appear at the inner region of the duct cross section because higher-order radial modes were excited. Although no more than two higher-order radial modes were generated, the modal detection method based on flush-mounted microphone data was able to determine the spinning modes inside of the duct with a high degree of accuracy. Tests under other test parameters were carried out and similar accuracy was obtained in each test result.

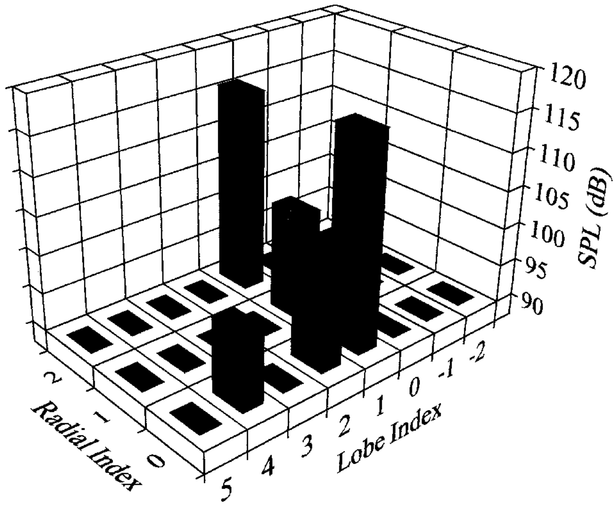

Fig. 6 Result of modal decomposition on spinning modes measured by the flush-mounted microphones.

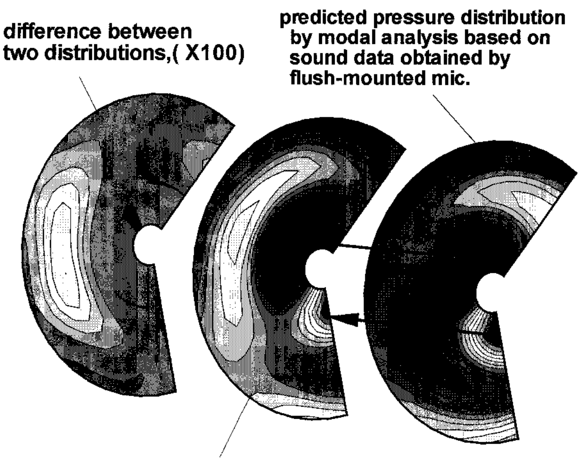

Fig. 7 Comparison of the pressure distribution in the duct measured by the traversing probe microphone with the distribution based on modal analysis of measurements from flush-mounted microphones.

D. Noise Measurements of a Ducted Fan

Before beginning the ANC tests, we examined the properties of fan noise under several sets of operating conditions. Similar studies have limited operating conditions to reduce the noise level caused by a lack of the acoustic power of the secondary sound source.[9,10] At a fan speed over 5500 rpm, the SPL of the fan tone reached to the extent more than 130 dB, which is too large to be canceled by the acoustic driver units. Considering the modal cutoff frequency and the sound power level available for the secondary sound source, we selected fan speeds of 4500 and 4125 rpm. Table 2 lists test parameters for the ANC of fan tones.

The sound spectrum obtained by the reference microphone fixed on the duct surface is shown in Fig. 8. The fan speed was 4500 rpm, and a corresponding 1200 Hz of the first blade-passage frequency (1-BPF) was retained during the tests. Broadband noise above 4000 Hz is much smaller than the 1-BPF components and disappears outside the duct inlet.

At a fan speed of 4500 rpm, the flush-mounted microphones measured fan noise and modal detection was conducted based on the measured data. The result of modal decomposition at 1-BPF (1200 Hz) is shown in Fig. 9. In this study, because only one ring array of secondary sound sources is installed in the axial direction of the duct, it is impossible to generate an arbitrary spinning mode with higher radial distributions by the array. The modal decomposition and ANC test focused only on spinning modes with the lowest radial order. In the figure, a spinning mode with one lobe, (−1,0) mode, is noted to be

Table 2 Test parameters for ANC

Case	Location of error microphone	Fan speed, rpm	Spinning modes (cut-on)
A	Outside the duct inlet (10 deg/1.1 m away)	4500	(−1,0), (−1,1), (−1,2)
B	On the duct inner wall	4125	(−1,0), (−1.1), (−1.2)

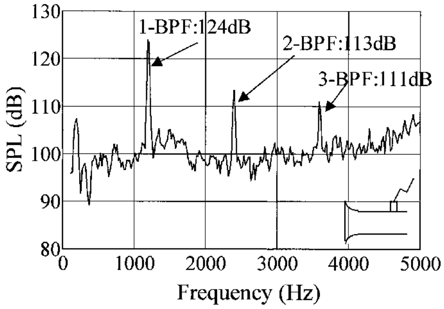

Fig. 8 Fan noise measured by a flush-mounted microphone in the duct (fan speed: 4500 rpm).

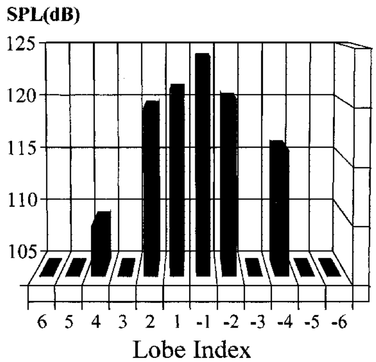

Fig. 9 Modal decomposition of spinning modes at 1-BPF (1200 Hz) measured at 4500 rpm of fan speed.

dominant. The excitation of the (−1,0) mode is also suggested by the numbers of fan blades and rods. In the ANC tests, we tried to reduce only the (−1,0) mode for the purpose of validating the ANC feasibility with the waveform synthesis. Similar tendency could be obtained at a fan speed of 4125 rpm (1-BPF = 1100 Hz).

IV. ANC Tests

A. Results of ANC Tests

ANC system performance was tested at fixed fan speeds of 4500 and 4125 rpm. At first, the input signals that would form an antiphased spinning mode are computed and transmitted to the acoustic driver units. The antiphased spinning mode is controlled in magnitude and phase, referring to the trigger signal sensed by the optical fiber sensor when a fan blade passes by the sensor. The trigger signal is delayed at the signal-delay controller and transmitted to external input of the 16-channel signal generator. At the delay controller, the delayed time is adjusted so that the output of the error microphone is minimized. After the optimum magnitude and phase of the antiphased-spinning mode are adjusted, the SPL outside of the duct inlet is measured by the boom microphone to evaluate the noise reduction level caused by the ANC system.

As for the location of the error microphone, two locations were examined. One location was outside of the duct inlet, which is not practical for aircraft application. In this test, a microphone is located at the polar angle of 10 deg on the boom path. The ANC test at a fan speed of 4500 rpm was performed with the error microphone at this location (Case-A). Another location was selected on the duct surface (Case-B). In Case-B, the spinning modes produced by the secondary sound source are expected to coincide with the spinning modes caused by the fan. The coincidence of both spinning modes can lead to the noise reduction outside the duct inlet without spillover.

In Fig. 10, sound spectra outside the duct inlet are shown with ANC and without ANC in Case-A. The measurement position was at the polar angle of 10 deg, where the error microphone was located. It is evident that the SPL of 1-BPF was decreased by 13 dB with the ANC. The SPL outside the duct inlet is plotted vs a corresponding polar angle in Fig. 11. At a fan speed of 4500 rpm, it was found that the maximum noise reduction was achieved at the location of the error microphone. Noise reduction at the peak radiation angle was only 5 dB. It can also be seen that spillover resulting from the secondary sound source appeared at the two polar angles of 0 and 90 deg.

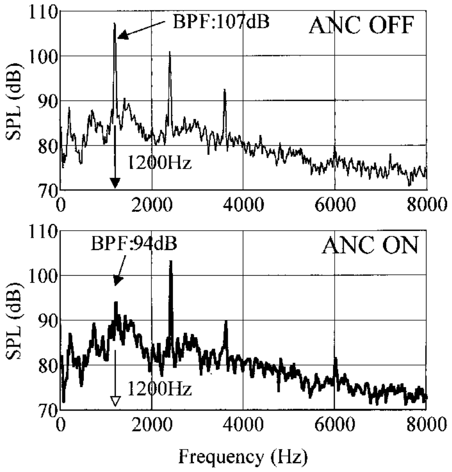

Fig. 10 Comparison of sound pressure levels in far field with ANC and without ANC measured by a microphone at a polar angle of 10 deg (Case-A: fan speed 4500 rpm).

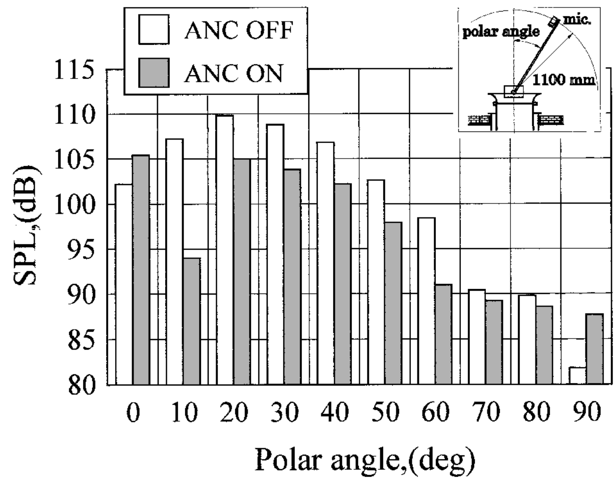

Fig. 11 SPL at BPF in the far field with and without ANC (Case-A: error sensor in far field at 10 deg, fan speed 4500 rpm).

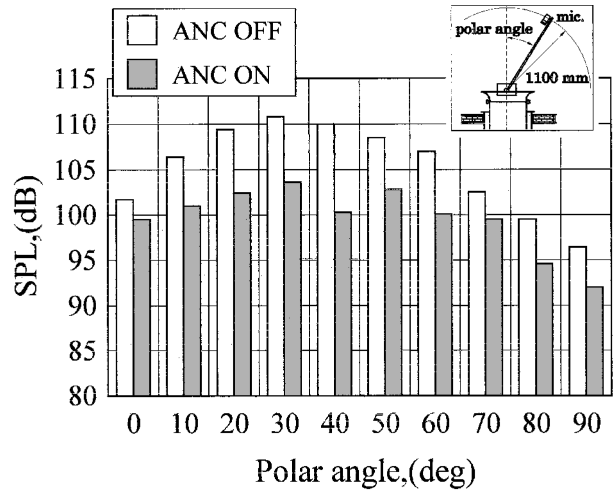

Fig. 12 SPL at 1-BPF in the far field with and without ANC (Case-B: error sensor flush mounted in duct, fan speed 4125 rpm).

The results in Case-B at a fan speed of 4125 rpm, in which a flush-mounted microphone was used as an error sensor, provided more uniform control, as seen in Fig. 12. The SPL of 1-BPF is reduced in all directions outside the duct inlet. This indicates that ANC using the waveform technique can succeed in reducing the fan tone without spillover. In doing so, the spinning mode made by the secondary sound source coincides with the spinning mode caused by the fan in antiphase. This suggests that the ANC performance can be further improved using the waveform technique, providing quicker signal processing and more accurate modal detection.

B. Additional Technical Issues

At the present stage, additional technical issues still need to be resolved to further reduce fan noise. One issue is in reducing the higher harmonic components of fan tones. The simultaneous reduction of tones in 1-BPF and harmonics requires superimposed signal inputs into each channel of the driver units. The computed arbitrary signals would compose spinning modes suitable for canceling fan tones containing higher harmonics. For noise reduction of higher radial modes, a set of sound source array in axial direction is being designed and fabricated as shown in Fig. 13. The acoustic power of the secondary sound source is also an important issue for ANC of fan noise at a higher fan speed. Radiation efficiency as well as acoustic power also should be improved for practicing ANC. For example, a piezoelectric actuator attached on a thin disk is expected in the next ANC test.

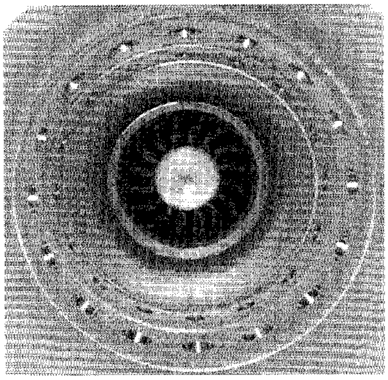

Fig. 13 Photograph taken in the duct. The duct has been improved for installing another array of secondary sound sources in different axial positions. In front of the former array, a new array is fabricated. The excitor rods are now removed.

V. Summary

For the purposes of investigating ANC feasibility, the waveform technique was applied to a ducted model fan. At first, we developed waveform generation and modal detection systems and then examined their performance. Next, the ANC of a fan tone was tested with both systems combined. The major observations are summarized next.

1) The waveform generation system produced desired spinning modes with lobes ranging from 1 to 7. As for a spinning mode with one lobe, it was confirmed that the produced spinning modes were able to cancel the original spinning modes caused by the model fan.

2) The driving frequency of the waveform generation system is restricted low enough to prevent the modal alliancing and the undesired higher radial modes.

3) Comparing the reference data measured by a probe microphone, it was found that the modal detection system composed of the flush-mounted microphones could determine spinning modes with a high accuracy even if higher radial modes were involved. However, because of the lack of secondary sound sources, the performance of the system could not validate for spinning modes with more than eight lobes.

4) When the error microphone was located on the duct surface, the sound pressure level of 1-BPF could be reduced in all directions outside the duct inlet, which ranges from 2 to 10 dB. Although the experimental data are limited, this fact suggests that the ANC using the waveform synthesis could achieve a reduction in noise without spillover because of the secondary sound source.

5) Additional technical issues for further improvement remain, such as the simultaneous reduction of the higher-order components and the lack of acoustic power available for noise cancellation.

Acknowledgments

This research was sponsored, in part, by the Environment Agency of Japan. This financial support is gratefully acknowledged. The technical advice by Katsumi Takeda and Mitsuo Gomi, Senior Researchers of National Aerospace Laboratory in Japan, with regard to sound measurement is also gratefully acknowledged.

References

[1]Tyler, J. M., and Sofrin, T. G., "Axial Flow Compressor Noise Studies," *Society of Automotive Engineers Transactions*, Vol. 70, 1962, pp. 309–332.

[2]Morfey, C. L., "Rotating Pressure Patterns in Ducts: Their Generation and Transmission," *Journal of Sound and Vibration*, Vol. 1, 1964, pp. 60–87.

[3]Mugridge, B. D., "The Measurement of Spinning Acoustic Modes Generated in an Axial Flow Fan," *Journal of Sound and Vibration*, Vol. 10, No. 2, 1969, pp. 227–246.

[4]Plumblee, H. E., and Dean, P. D., "Sound Measurements Within and in the Radiated Field of an Annular Duct with Flow," *Journal of Sound and Vibration*, Vol. 28, No. 4, 1973, pp. 715–735.

[5]Pickett, G. F., Wells, R. A., and Love, R. A., "Method of Fan Sound Mode Structure Determination Computer Program User's Manual Modal Calculation Program," NASA CR-135295, Aug. 1977.

[6]Joppa, P. D., "An Acoustic Mode Measurement Technique," AIAA Paper 84-2337, Oct. 1984.

[7]Nakamura, Y., and Isomura, K., "Detection of Fan Acoustic Mode," AIAA Paper 87-2700, Oct. 1987.

[8]Kraft, R. E., and Kontos, K. B., "Theoretical Implications of Active Noise Control for Turbofan Engines," AIAA Paper 93-4355, Oct. 1993.

[9]Thomas, R. H., Burdisso, R. A., Fuller, C. R., and O'Brien, W. F., "Active Control of Fan Noise from a Turbofan Engine," AIAA Paper 93-0597, Jan. 1993.

[10]Burdisso, R. A., Thomas, R. H., Fuller, C. R., and O'Brien, W. F., "Active Control of Spinning Acoustic Modes from a Turbofan Engine," AIAA Paper 94-0361, Jan. 1994.

[11]Thomas, R. H., Burdisso, R. A., and Lane, S. A., "Time-Averaged Active Controller for Turbofan Engine Fan Noise Reduction," *Journal of Aircraft*, Vol. 33, No. 3, 1996, pp. 524–531.

[12]Thomas, R. H., Burdisso, R. A., Fuller, C. R., and O'Brien, W. F., "Active Control of Fan Noise from a Turbofan Engine," *AIAA Journal*, Vol. 32, No. 1, 1994, pp. 23–30.

[13]Sutliff, D. L., and Nagel, R. T., "Active Control of Far-Field Noise from a Ducted Propeller," AIAA Paper 93-4356, Oct. 1993.

[14]Koopman, G. H., Neise, W., and Chen, W., "Active Noise Control to Reduce the Blade Tone Noise of Centrifugal Fans," *Proceedings of Inter Noise-88*, Aug. 1988, pp. 801–804.

[15]Stevens, J., and Ahuja, K., "The State-of-the-Art in Active Noise Control," AIAA Paper 90-3924, Oct. 1990.

[16]Ishii, T., Kobayashi, H., and Oinuma, H., "Waveform Technique for Reduction of Tones Radiated from a Ducted Fan," AIAA Paper 97-1664, May 1997.